SCIENTIFIC REPORTS

OPEN

Uniform magnetic force impact on water based nanofluid thermal behavior in a porous enclosure with ellipse shaped obstacle

Received: 3 August 2018
Accepted: 18 December 2018
Published online: 04 February 2019

M. Sheikholeslami[1,2], Zahir Shah[3], Ahmad Shafee[4,5], Ilyas Khan[6] & Iskander Tlili[7]

In the present research, aluminum oxide- water (Al_2O_3-H_2O) nanofluid free convection due to magnetic forces through a permeable cubic domain with ellipse shaped obstacle has been reported. Lattice Boltzmann approach is involved to depict the impacts of magnetic, buoyancy forces and permeability on nanoparticles migration. To predict properties of Al_2O_3- water nanofluid, Brownian motion impact has been involved. Outcomes revels that considering higher magnetic forces results in greater conduction mechanism. Permeability can enhance the temperature gradient.

By suggesting nanoparticles from nanoscience as useful working fluid, thermal performance enhances. Nano sized metallic particles are dispersed into common fluid to generate such fluid. Nanofluids must be utilized to augment the conduction and can be more stable with better mixing[1,2]. Nano science can suggest appropriate working fluid to reach thermal efficiency enhancement[3–6]. The furthermost current publications on nanofluids with new applications can be demonstrated in[7–12]. Kumar *et al.*[13] involved the Brownian motion impact on characteristics of nanoparticles in bioconvective flow. Irfan *et al.*[14] displayed the roles of chemical terms on transient energy equation. Ahmed *et al.*[15] illustrated the carbon nanotubes flow between Riga sheets in existence of viscous dissipation. Kumar *et al.*[16] employed the non-Fourier heat flux model for investigation of magnetic force effect on Carreau fluid convective transient flow. Ali *et al.*[17] demonstrated hidden events during magnetohydrodynamic (MHD) migration in a permeable media. Soomro *et al.*[18] employed Finite difference method (FDM) for dual solution of nanoparticle migration over a cylinder. They used water as pure fluid. Reddy *et al.*[19] depicted the impact of magnetic terms on fluid flow along a sheet considering heat sink. Raizah *et al.*[20] illustrated the power law nanofluid natural convection inside a titled permeable duct. The furthermost recent articles about Nano sized particles transportation by involving various methods were reported by Shah *et al.*[9,21,22]. Choosing active working fluid becomes popular subject in recent decade[23–51].

The main aim of current research is to simulate and examine nanoparticles migration within a cubic porous cavity under the influence of constant magnetic force. Hydrothermal behaviors for various permeability, Lorentz and buoyancy forces are mainly focused and shown through graph.

Geometry Explanation

Figure 1 displays the permeable cubic cavity which is full of alumina. Cold, adiabatic and hot surfaces are depicted in this graph. One direction magnetic force has been involved. ($\theta_z = 0.5\,\pi = \theta_x$).

Simulation by Mesoscopic Method

Mesoscopic method. To find the temperature and velocity, distribution functions were used namely (g and f). Boltzmann equations help to find functions g and f. According to assumptions exist in[38], we have:

[1]Department of Mechanical Engineering, Babol Noshirvani University of Technology, Babol, Iran. [2]Renewable energy systems and nanofluid applications in heat transfer Laboratory, Babol Noshirvani University of Technology, Babol, Iran. [3]Department of Mathematics, Abdul Wali Khan University, Mardan, KP, Pakistan. [4]FAST, University Tun Hussein Onn Malaysia, 86400, Parit Raja, Batu Pahat, Johor State, Malaysia. [5]Public Authority of Applied Education and Training, College of Technological Studies, Applied Science Department, Shuwaikh, Kuwait. [6]Faculty of Mathematics and Statistics, Ton Duc Thang University, Ho Chi Minh City, Vietnam. [7]Energy and Thermal Systems Laboratory, National Engineering School of Monastir, Street Ibn El Jazzar, 5019, Monastir, Tunisia. Correspondence and requests for materials should be addressed to I.K. (email: ilyaskhan@tdt.edu.vn)

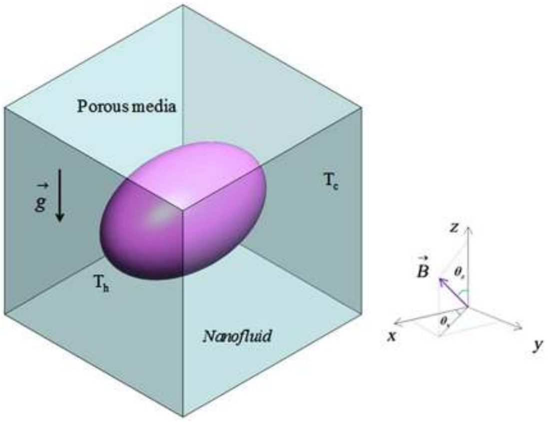

Figure 1. Current porous cubic cavity.

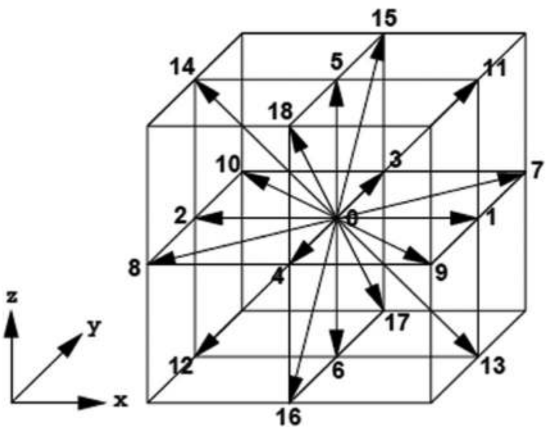

Figure 2. Diagram of D_3Q_{19} model.

	$\sigma(\Omega\cdot m)^{-1}$	k(W/m.k)	C_p(j/kgk)	$\rho(kg/m^3)$
Pure water	0.05	0.613	4179	997.1
Al_2O_3	10^{-12}	25	765	3970

Table 1. Properties of *Water*, Al_2O_3.

Coefficient values	Al_2O_3—Water
a_6	−298.19819084
a_7	−34.532716906
a_8	−3.9225289283
a_9	−0.2354329626
a_{10}	−0.999063481
a_1	52.813488759
a_2	6.115637295
a_3	0.6955745084
a_4	4.174555527E-02

Table 2. Related coefficient for alumina.

Mesh size	51 × 51 × 51	61 × 61 × 61	71 × 71 × 71	81 × 81 × 81	91 × 91 × 91
Nu_{ave}	0.13622	0.14805	0.15061	0.15073	0.15097

Table 3. Nu_{ave} over the hot surface with various grid sixes when $Da=100$, $\phi=0.04$, $Ra=10^5$, and $Ha=60$.

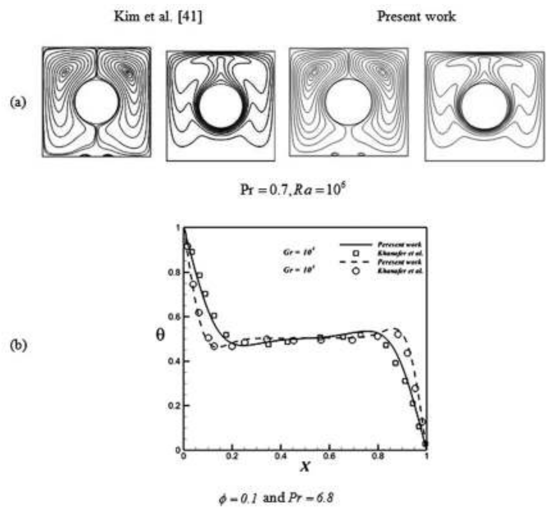

Figure 3. Verification of current LBM code for (**a**) free convention[40]; (**b**) nanofluid flow[41].

$$\Delta t\ \tau_C^{-1}[-g_i(x,\ t) + g_i^{eq}(x,\ t)] = g_i(x + \Delta t\ c_i,\ t + \Delta t) - g_i(x,\ t) \tag{1}$$

$$\Delta t\ \tau_v^{-1}[-f_i(x,\ t) + f_i^{eq}(x,\ t)] + f_i(x,\ t) + \Delta t c_i F_k = f_i(x + \Delta t\ c_i,\ t + \Delta t) \tag{2}$$

Here τ_c, Δt, τ_v and c_i are, relaxation time for T, time step, relaxation time for u and lattice velocity. D_3Q_{19} model is good method for such problem (as shown in Fig. 2):

$$c_i = \begin{pmatrix} 0 & 0 & 0 & 0 & -1 & -1 & -1 & -1 & 1 & 1 & 1 & 0 & 0 & 0 & 0 & -1 & 1 & 0 \\ -1 & -1 & 1 & 1 & 0 & -1 & -1 & 1 & 0 & -1 & 1 & 0 & 0 & -1 & 1 & 0 & 0 & 0 \\ -1 & 1 & -1 & 1 & -1 & 0 & 0 & 0 & 1 & 0 & 0 & -1 & 1 & 0 & 0 & 0 & 0 & 0 \end{pmatrix} \tag{3}$$

g_i^{eq} & f_i^{eq} are:

$$g_i^{eq} = w_i T\left[1 + \frac{c_i.\ u}{c_s^2}\right] \tag{4}$$

$$f_i^{eq} = \left[\frac{1}{2}\frac{(c_i.\ u)^2}{c_s^4} - \frac{1}{2}\frac{u^2}{c_s^2} + 1 + \frac{c_i.\ u}{c_s^2}\right] w_i \rho \tag{5}$$

$$w_i = \{i = 7{:}\ 18 \quad 1/36; \quad i = 0 \quad 1/3; \quad i = 1{:}\ 6 \quad 1/18\} \tag{6}$$

Body forces can calculate as:

$$\begin{aligned} F &= F_y + F_z + F_x \\ F_y &= \begin{aligned}[t] &3Aw_i\rho[-(-\sin(2\theta_z)\sin(\theta_x)(0.5)w + v\cos^2(\theta_z)) \\ &+(-v\cos^2(\theta_x)\sin^2(\theta_z) + 0.5u\ \sin(2\theta_x)\sin^2(\theta_z))] - 3BB\ w_i\rho v, \end{aligned} \\ F_x &= 3w_i A\rho[-\sin(\theta_x)(-v\ \sin^2(\theta_z)\cos(\theta_x) + \ \sin(\theta_x)u\ \sin^2(\theta_z)) \\ &\quad -\left(u\ \cos^2(\theta_z) + w\ \cos(\theta_x)\left(\frac{1}{2}\right)\sin(2\theta_z)\right)\Bigg] - BB(3)\rho w_i u, \\ F_z &= 3w_i\rho\Bigg[A\ \cos(\theta_x)\left(-\cos(\theta_x)\sin^2(\theta_z)w + \left(\frac{u}{2}\right)\cos(2\theta_z)\right) \\ &\quad + \sin(\theta_x)A\left(-\sin(\theta_x)\sin^2(\theta_z)w + \ \sin(2\theta_z)\frac{v}{2}\right) + \beta(T - T_m)g_z\Bigg] - BB(3w_i)w\rho, \\ Ha &= LB_0\sqrt{\frac{\sigma}{\mu}}, \quad A = Ha^2\mu L^{-2}, \\ Da &= \frac{K}{L^2}, \quad BB = \frac{\upsilon}{Da\ L^2} \end{aligned} \tag{7}$$

To calculate scholars we have:

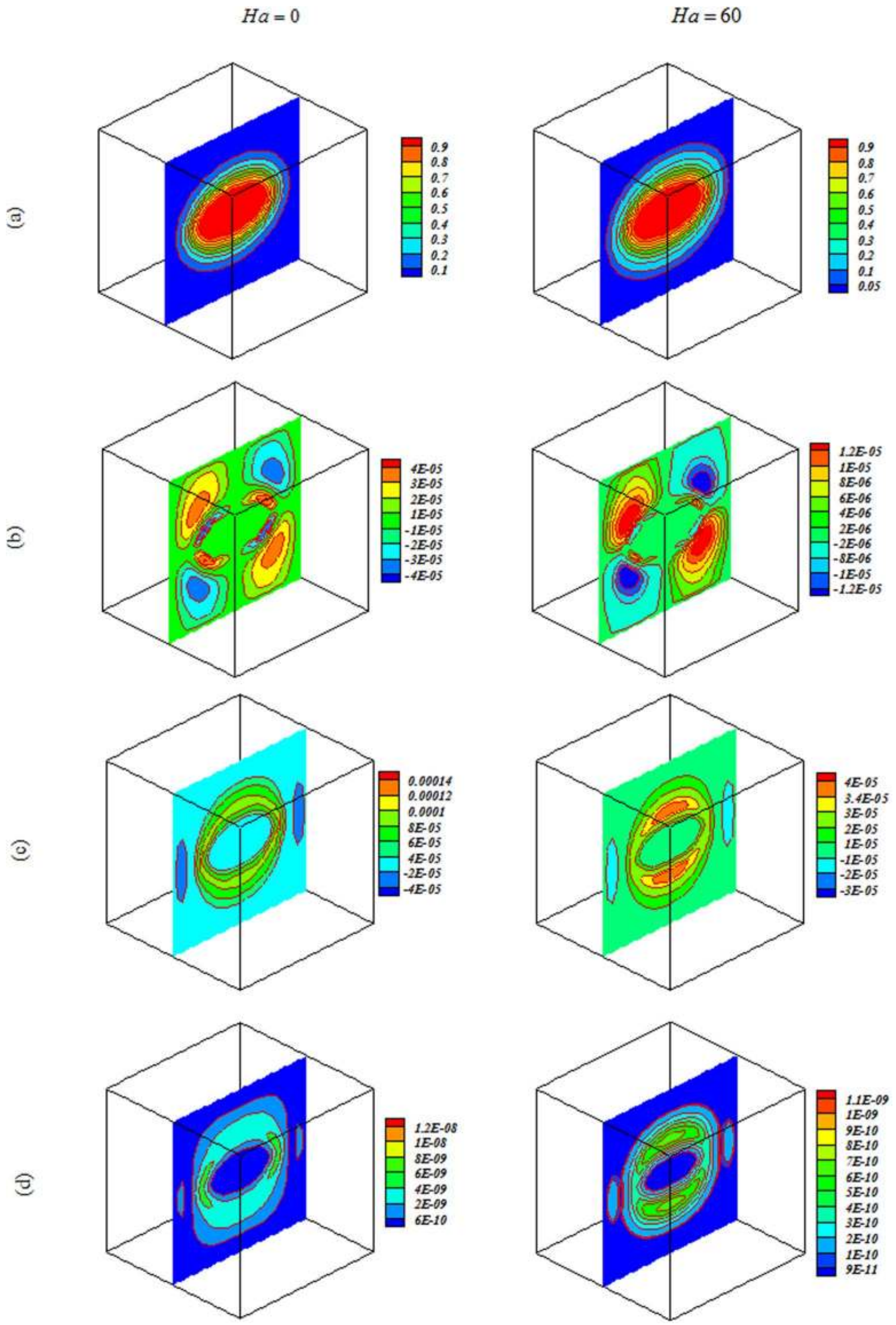

Figure 4. Impacts of magnetic forces on (**a**) isotherm, (**b**) x velocity, (c) z velocity, (**d**) isokinetic energy at $Y=y/L=0.5$ when $\phi=0.04$, $Da=0.001$, $Ra=10^3$.

$$\begin{aligned} &\text{Flow density: } \rho = \sum_i f_i, \\ &\text{Momentum: } \rho \mathrm{u} = \sum_i \mathrm{c}_i f_i, \\ &\text{Temperature: } T = \sum_i g_i. \end{aligned} \tag{8}$$

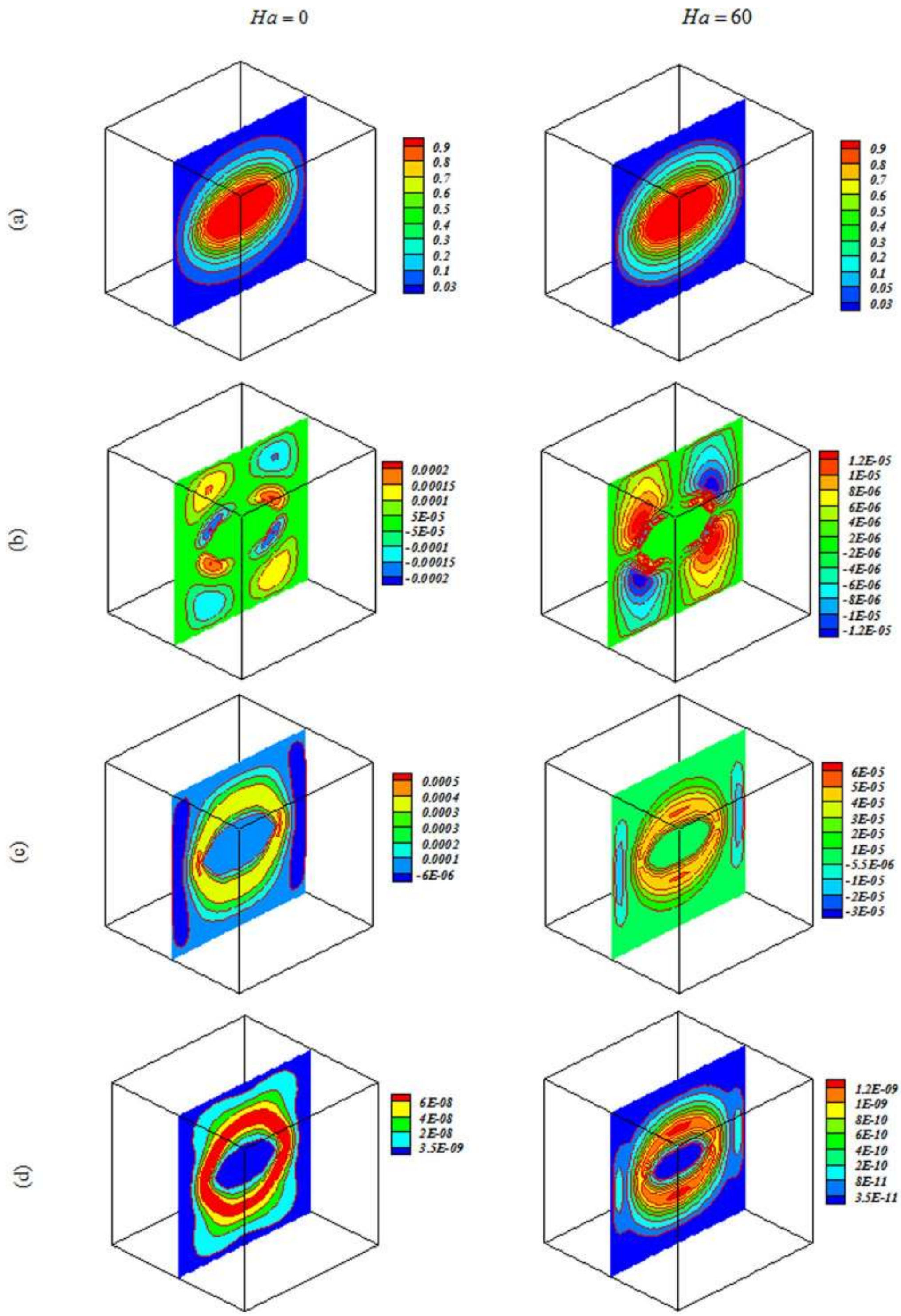

Figure 5. Impacts of magnetic forces on (**a**) isotherm, (**b**) x velocity, (**c**) z velocity, (**d**) isokinetic energy at $Y = y/L = 0.5$ when $Ra = 10^3$, $Da = 100$, $\phi = 0.04$.

Working fluid. Density, $(\rho\beta)_{nf}$, $(\rho C_p)_{nf}$, σ_{nf}, μ_{nf} and k_{nf} are ([39]):

$$\frac{\rho_{nf}}{\rho_f} = -\phi + \frac{\rho_s}{\rho_f}\phi + 1, \tag{9}$$

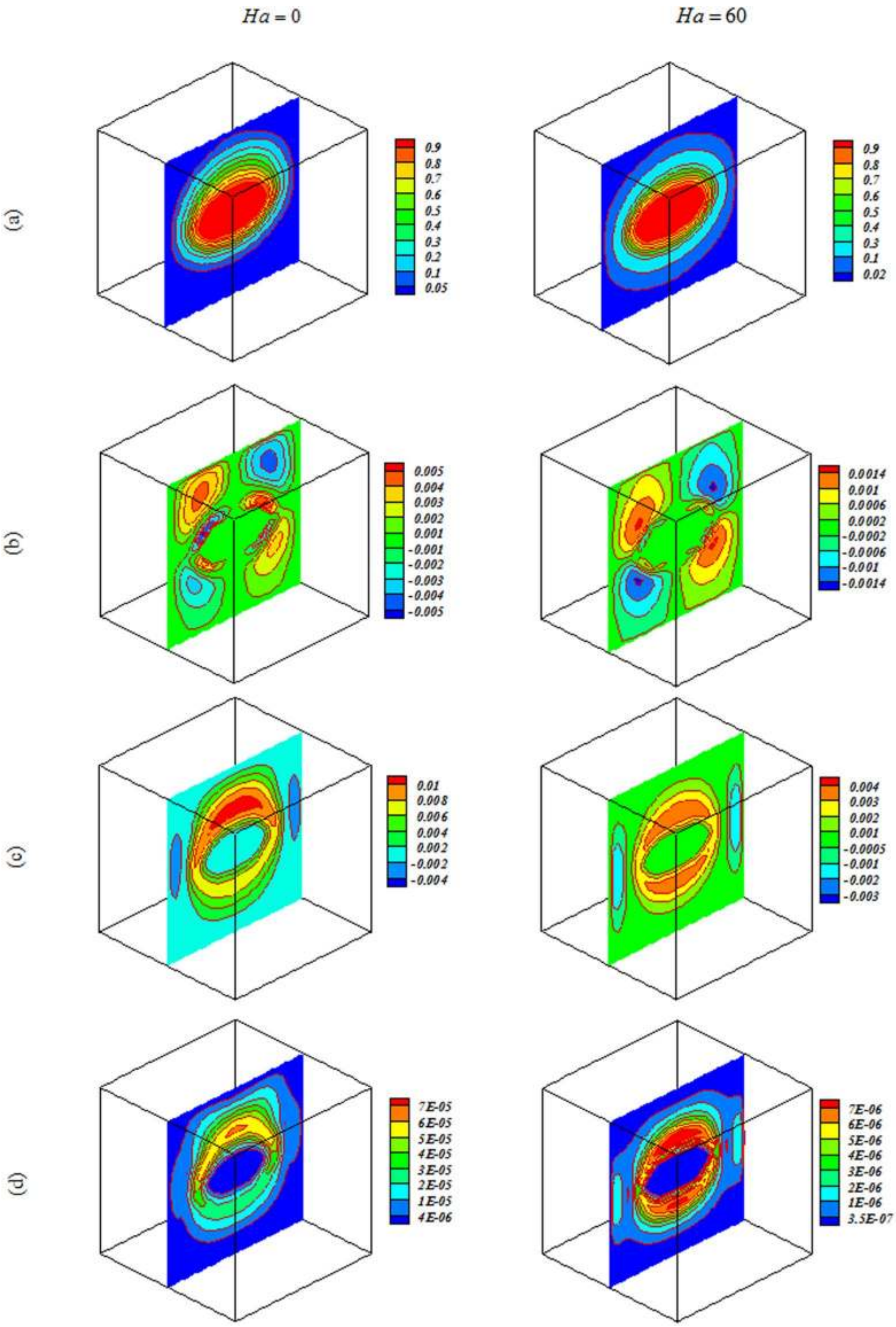

Figure 6. Impacts of magnetic forces on (**a**) isotherm, (**b**) x velocity, (**c**) z velocity, (**d**) isokinetic energy at $Y = y/L = 0.5$ when $Ra = 10^5$, $Da = 0.001$, $\phi = 0.04$.

$$(\rho\beta)_{nf} = \phi(\rho\beta)_s + (1 - \phi)(\rho\beta)_f \tag{10}$$

$$\left(\rho C_p\right)_{nf} / \left(\rho C_p\right)_f = -\phi + 1 + \left(\rho C_p\right)_s / \left(\rho C_p\right)_f \phi \tag{11}$$

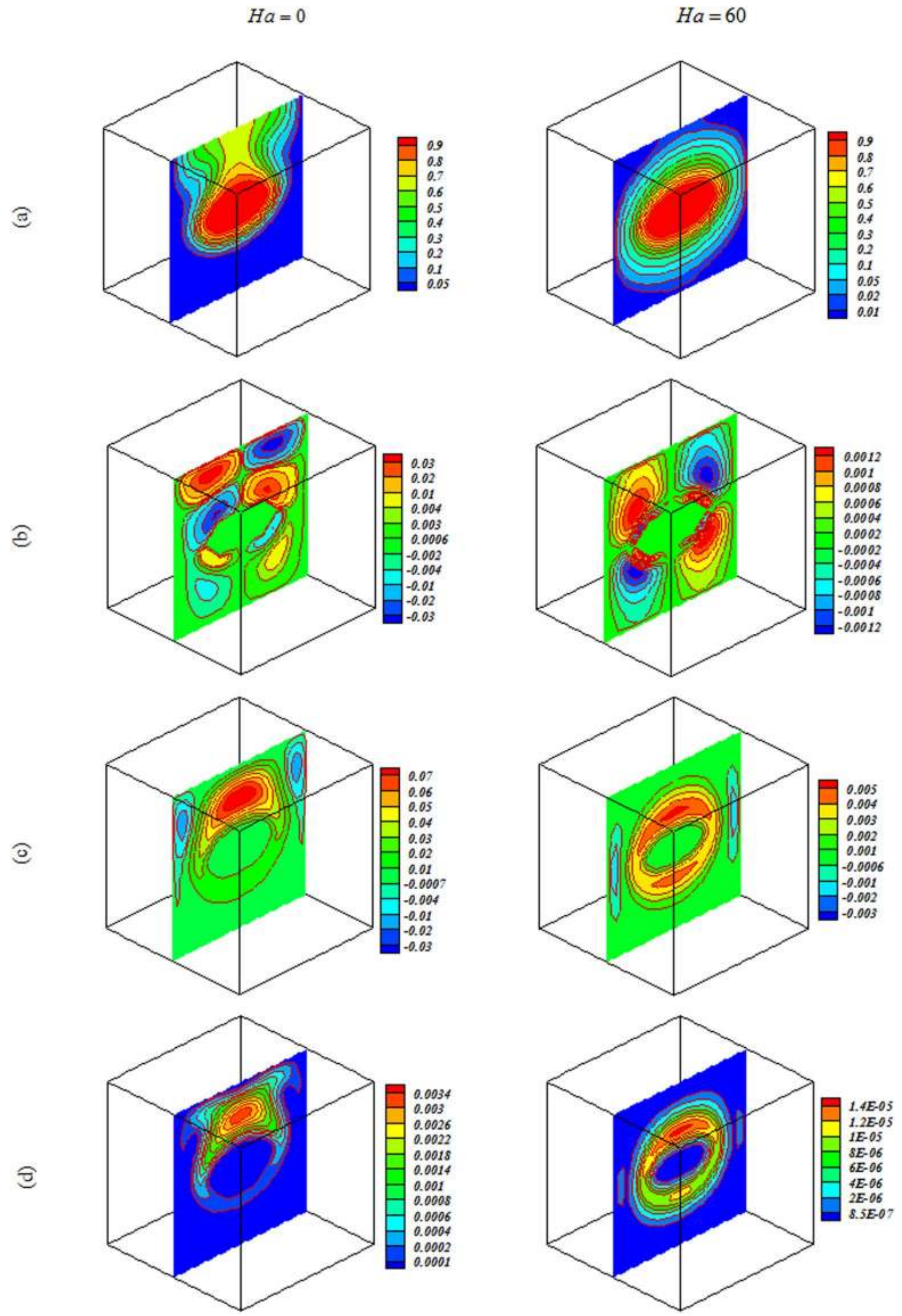

Figure 7. Impacts of magnetic forces on (**a**) isotherm, (**b**) x velocity, (**c**) z velocity, (**d**) isokinetic energy at $Y = y/L = 0.5$ when $Ra = 10^5$, $Da = 100$, $\phi = 0.04$.

$$\frac{\sigma_{nf}}{\sigma_f} = 1 + \left(\frac{(\Delta + 2) - \phi(\Delta - 1)}{3\phi(-1 + \Delta)}\right)^{-1}, \ \Delta = \sigma_s/\sigma_f \tag{12}$$

$$\mu_{nf} = \frac{\mu_f}{(1 - \phi)^{2.5}} + \frac{\mu_f}{\Pr}\frac{k_{Brownian}}{k_f} \tag{13}$$

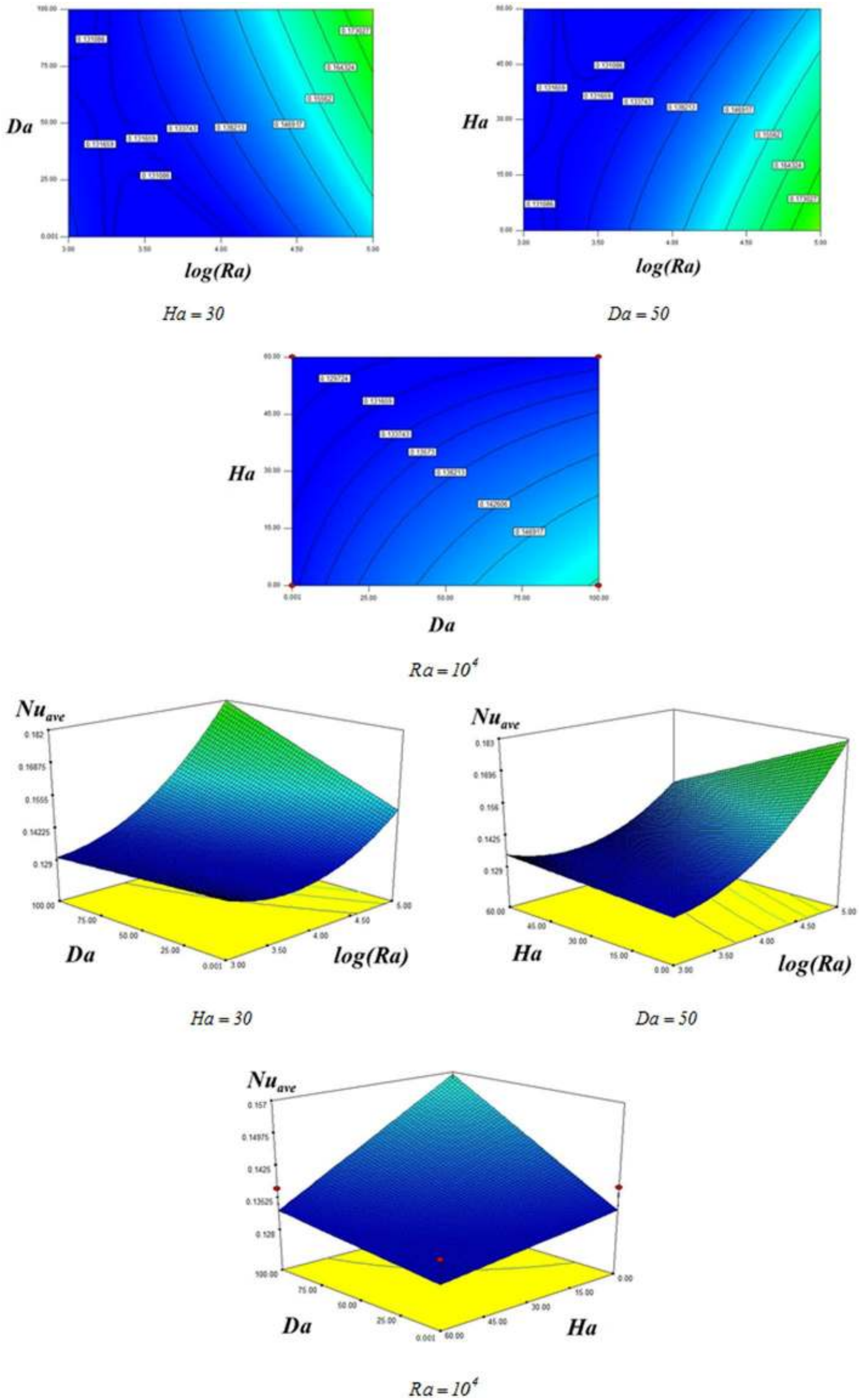

Figure 8. Various values of Nu_{ave} for different Ra, Da, Ha.

$$\frac{k_{nf}}{k_f} = 1 + 5 \times 10^4 g'(\phi, T, d_p)\phi\rho_f c_{p,f}\sqrt{\frac{\kappa_b T}{d_p \rho_p}} + \frac{3\left(-1 + \frac{k_p}{k_f}\right)\phi}{\left(\frac{k_p}{k_f} + 2\right) - \left(\frac{k_p}{k_f} - 1\right)\phi},$$
$$R_f = 4 \times 10^{-8} km^2/W,\ \ R_f = -d_p(1/k_p - 1/k_{p,eff}),$$
$$g'\left(\phi, d_p, T\right) = Ln(T)\left(a_1 + a_3 Ln(\phi) + Ln\left(d_p\right)^2 a_5 + a_2 Ln\left(d_p\right) + a_4 Ln\left(d_p\right) Ln(\phi)\right)$$
$$+\left(a_8 Ln(\phi) + Ln\left(d_p\right) a_7 + a_6 + a_{10} Ln\left(d_p\right)^2 + Ln\left(d_p\right) a_9 Ln(\phi)\right) \tag{14}$$

Tables 1 and 2[39] can be used to find needed parameters. Nu_{ave} and Nu_{loc} over the hot surface are:

$$Nu_{loc} = -\frac{k_{nf}}{k_f}\frac{\partial T}{\partial X}\bigg|_{X=0} \quad \text{and} \quad Nu_{ave} = \int_0^1\int_0^1 Nu\ dYdZ \tag{15}$$

The fluid kinetic energy is:

$$E_c = 0.5[(w)^2 + (v)^2 + (u)^2] \tag{16}$$

Mesh Independency and Validation

No alter should be seen in outputs by changing mesh sizes. So, various sizes must be employed. As an example, we presented Table 3. Figure 3 illustrates the agreement of Lattice Boltzmann Method (LBM)[40,41]. Also, previous paper[42] indicates that this code is verified for MHD flow.

Results and Discussion

Water-Aluminum oxide mixture hydrothermal behavior in a permeable three dimensional domain was modeled with mesoscopic method. Numerical outputs are depicted the variations of magnetic force ($Ha = 0$ to 60), buoyancy term ($Ra = 10^3$, 10^4 and 10^5) and Darcy number ($Da = 0.001$ to 100).

Nanofluid behavior with change of Ra, Ha and Da are displayed in Figs 4–7. In cases with low Ra and Da, convection mode is not strong enough to change flow style and isotherms has shape of geometry. Convection enhancements with increase of permeability and isotherms convert to complex shape. Thermal plume appears as a result of strong convection mode. Employing magnetic forces makes conduction to be more sensible and thermal plumes vanish. Due to reduction effect of Ha on velocity, E_c detracts with rise of Ha. By augment of buoyancy force, main vortex stretch in z direction and convection mode rises.

Changes in Nu_{ave} due to altering variables are illustrated in Fig. 8. Equation (17) is extracted for Nu_{ave}:

$$\begin{aligned} Nu_{ave} &= 0.14 + 0.017\log(Ra) + 6.8\times10^{-3}Da - 7.2\times10^{-3}Ha + 9\times10^{-3}(\log(Ra))(Da) \\ &\quad - 9\times10^{-3}(\log(Ra))(Ha) - 4.7\times10^{-3}(Da)(Ha) + 0.012(\log(Ra))^2. \end{aligned} \tag{17}$$

Due to augment in temperature gradient with rise of permeability and buoyancy terms, Nu_{ave} is enhancing function of Da, Ra. Furthermore, conduction mode boosts with augment of Hartmann number. Thus, Nu_{ave} detracts with rise of magnetic force.

Conclusions

In the current article, uniform magnetic force impacts on momentum equations were considered in a 3D porous enclosure. Mesoscopic approach was applied to analyze alumina nanofluid in these conditions. Brownian motion impact can changes the properties of working fluid. LBM was involved to report the impacts of Ha, Ra, Da on nanofluid behavior. Outcomes display that interaction of nanoparticles augments with augment of Da,Ra. Isotherms become less complex with applying magnetic force.

References

1. Wong, K. F. V. & Leon, O. D. Applications of nanofluids: current and future. *Adv. Mech. Engng*. 1–11 (2010).
2. Dianchen, L., Ramzan, M., Naeem, U., Chung, J. D. & Umer, F. A numerical treatment of radiative nanofluid 3D flow containing gyrotactic microorganism with anisotropic slip, binary chemical reaction and activation energy. *Scientific Reports.* **7**, 17008 (2017).
3. Ul Haq, R., Nadeem, S., Khan, Z. H. & Noor, N. F. M. Convective heat transfer in MHD slip flow over a stretching surface in the presence of carbon nanotubes. *Physica B: Condensed Matter* **457**(15), 40–47 (2015).
4. Khairy, Z., Anuar, I. & Ioan, P. Boundary layer flow and heat transfer over a nonlinearly permeable stretching/shrinking sheet in a nanofluid. *Scientific Reports.* **4**, 4404 (2014).
5. Khan, I., Shah, N. A. & Dennis, L. C. A scientific report on heat transfer analysis in mixed convection flow of Maxwell fluid over an oscillating vertical plate. *Scientific Reports.* **7**, 40147 (2017).
6. Sidra, A., Khan, I., Zulkhibri, I., Mohd, Z. S. & Qasem, M. M. Heat transfer enhancement in free convection flow of CNTs Maxwell nanofluids with four different types of molecular liquids. *Scientific Reports* **2445**, 01358–3 (2017).
7. Sheikholeslami, M. *et al.* Nanofluid heat transfer augmentation and exergy loss inside a pipe equipped with innovative turbulators. *International Journal of Heat and Mass Transfer* **126**, 156–163 (2018).
8. Kumar, KA., Sugunamma, V., Sandeep, N. Simultaneous solutions for MHD flow of Williamson fluid over a curved sheet with non-uniform heat source/sink. *Heat Transfer Research* (2018).
9. Shah, Z., Islam, S., Gul, T., Bonyah, E. & Khan, M. A. Three dimensional third grade nanofluid flow in a rotating system between parallel plates with Brownian motion and thermophoresis effects. *Results Phys.* **10**, 36–45 (2018).
10. Yuan, M., Fenghua, S. & Yangzhi, C. Supercritical fluid synthesis and tribological applications of silver nanoparticle-decorated graphene in engine oil nanofluid. *Scientific Reports* **31246**, 31246 (2016).
11. Sheikholeslami, M. Finite element method for PCM solidification in existence of CuO nanoparticles. *Journal of Molecular Liquids* **265**, 347–355 (2018).
12. Sheikholeslami, M. Solidification of NEPCM under the effect of magnetic field in a porous thermal energy storage enclosure using CuO nanoparticles. *Journal of Molecular Liquids* **263**, 303–315 (2018).
13. Kumar, K. A., Sugunamma, V., Sandeep, N., Reddy, J. V. R. Impact of Brownian motion and thermophoresis on bioconvective flow of nanoliquids past a variable thickness surface with slip effects. *Multidiscipline Modeling in Materials and Structures*, https://doi.org/10.1108/MMMS-02-2018-0023 (2018).
14. Irfan, M., Khan, M. & Khan, W. A. Impact of autocatalysis chemical reaction on nonlinear radiative heat transfer of unsteady 3D Eyring-Powell magneto-nanofluid flow. *Results in Physics* **10**, 107–117 (2018).
15. Ahmed, N., Adnan, Khan, U. & Mohyud-Din, S. T. Influence of Thermal Radiation and Viscous dissipation on Squeezed flow of Water between Riga Plates saturated with Carbon nanotubes. *Colloids and Surfaces A: Physicochemical and Engineering Aspects* **522**, 389–398 (2017).

16. Kumar, K. A., Ramadevi, B. & Sugunamma, V. Impact of Lorentz force on unsteady bio convective flow of Carreau fluid across a variable thickness sheet with non-Fourier heat flux model. *Defect and Diffusion Forum* **387**, 474–497 (2018).
17. Ali, F., Sheikh, N.A., Saqib, M. & Khan, A. Hidden Phenomena of an MHD Unsteady Flow in Porous Medium with Heat Transfer. *Journal of Nonlinear Science: Letter A*. 101–116 (2017).
18. Soomro, F. A., Zaib, A., Haq, R. U. & Sheikholeslami, M. Dual nature solution of water functionalized copper nanoparticles along a permeable shrinking cylinder: FDM approach. *International Journal of Heat and Mass Transfer* **129**, 1242–1249 (2019).
19. Reddy, J. V. R., Kumar, K. A., Sugunamma, V. & Sandeep, N. Effect of cross diffusion on MHD non-Newtonian fluids flow past a stretching sheet with non-uniform heat source/sink: A comparative study. *Alexandria engineering journal* (2017).
20. Raizah, Z. A. S., Aly, A. M. & Ahmed, S. E. Natural convection flow of a power-law non-Newtonian nanofluid in inclined open shallow cavities filled with porous media. *International Journal of Mechanical Sciences* **140**, 376–39 (2018).
21. Shah, Z., Islam, S., Ayaz, H. & Khan, S. Radiative Heat And Mass Transfer Analysis Of Micropolar Nanofluid Flow Of Casson Fluid Between Two Rotating Parallel Plates With Effects Of Hall Current. *ASME Journal of Heat Transfer*, 10.1115/1.4040415 (2018).
22. Shah, Z., Islam, S., Gul, T., Bonyah, E. & Khan, M. A. The electrical MHD and hall current impact on micropolar nanofluid flow between rotating parallel plates. *Results Phys.* **9**, 1201–1214, https://doi.org/10.1016/j.rinp.2018.01.064 (2018).
23. Kempannagari, A. K., Janke, V. R. R., Vangala, S. & Naramgari, S. Impact of frictional heating on MHD radiative ferrofluid past a convective shrinking surface. *Defect and Diffusion Forum* **378**, 157–174 (2017).
24. Shah, Z., Gul, T., Khan, A. M., Ali, I. & Islam, S. Effects of hall current on steady three dimensional non-newtonian nanofluid in a rotating frame with brownian motion and thermophoresis effects. *J. Eng. Technol.* **6**, 280–296 (2017).
25. Sheikholeslami, M. Numerical modeling of Nano enhanced PCM solidification in an enclosure with metallic fin. *Journal of Molecular Liquids* **259**, 424–438 (2018).
26. Sheikholeslami, M. Numerical investigation of nanofluid free convection under the influence of electric field in a porous enclosure. *Journal of Molecular Liquids* **249**, 1212–1221 (2018).
27. Sheikholeslami, M., Rokni & Houman, B. Numerical simulation for impact of Coulomb force on nanofluid heat transfer in a porous enclosure in presence of thermal radiation. *International Journal of Heat and Mass Transfer* **118**, 823–831 (2018).
28. Fengrui, S., Yuedong, Y. & Xiangfang, L. The Heat and Mass Transfer Characteristics of Superheated Steam Coupled with Non-condensing Gases in Horizontal Wells with Multi-point Injection Technique. *Energy* **143**, 995–1005 (2018).
29. Najwa, N., Norfifah, B., Norihan, M. A. & Anuar, I. Stagnation point flow and mass transfer with chemical reaction past a stretching/shrinking cylinder. *Scientific Reports* **4178**, 04178 (2014).
30. Sheikholeslami, M. Numerical approach for MHD Al2O3-water nanofluid transportation inside a permeable medium using innovative computer method. *Computer Methods in Applied Mechanics and Engineering.* **344**, 306–318, https://doi.org/10.1016/j.cma.2018.09.042 (2019).
31. Sheikholeslami, M., Khan, I. & Tlili, I. Non-equilibrium model for nanofluid free convection inside a porous cavity considering Lorentz forces. *Scientific Reports*, https://doi.org/10.1038/s41598-018-33079-6 (2018).
32. Sheikholeslami, M. Application of Darcy law for nanofluid flow in a porous cavity under the impact of Lorentz forces. *Journal of Molecular Liquids* **266**, 495–503 (2018).
33. Sheikholeslami, M., Li, Z. & Shafee, A. Lorentz forces effect on NEPCM heat transfer during solidification in a porous energy storage system. *International Journal of Heat and Mass Transfer* **127**, 665–674 (2018).
34. Syam, L. S. *et al*. Enhanced thermal conductivity and viscosity of nanodiamond-nickel nano composite nanofluids. *Scientific Reports* **4039**, 04039 (2014).
35. Fengrui, S. *et al*. Flow Simulation of the Mixture System of Supercritical CO2 & Superheated Steam in Toe-point Injection Horizontal wellbores. *Journal of Petroleum Science and Engineering* **163**, 199–210 (2018).
36. Sheikholeslami, M. New computational approach for exergy and entropy analysis of nanofluid under the impact of Lorentz force through a porous media. *Computer Methods in Applied Mechanics and Engineering* **344**, 319–333, https://doi.org/10.1016/j.cma.2018.09.044 (2019).
37. Sheikholeslami, M. Influence of magnetic field on Al2O3-H2O nanofluid forced convection heat transfer in a porous lid driven cavity with hot sphere obstacle by means of LBM. *Journal of Molecular Liquids* **263**, 472–488 (2018).
38. Sheikholeslami, M. Numerical simulation for solidification in a LHTESS by means of Nano-enhanced PCM. *Journal of the Taiwan Institute of Chemical Engineers* **86**, 25–41 (2018).
39. Soomro, F. A., Haq, R. U., Khan, Z. H. & Zhang, Q. Passive control of nanoparticle due to convective heat transfer of Prandtl fluid model at the stretching surface. *Chinese Journal of Physics* **55**(4), 1561–1568 (2017).
40. Yan, Y. Y. & Zu, Y. Q. Numerical simulation of heat transfer and fluid flow past a rotating isothermal cylinder — A LBM approach. *Int. J.Heat and Mass Transfer.* **51**, 2519–2536 (2008).
41. Sheikholeslami, M., Barzegar Gerdroodbary, M., Moradi, R., Shafee, A. & Li, Z. Application of Neural Network for estimation of heat transfer treatment of Al2O3- H2O nanofluid through a channel. *Computer Methods in Applied Mechanics and Engineering* **344**, 1–12, https://doi.org/10.1016/j.cma.2018.09.025 (2019).
42. Kim, B. S., Lee, D. S., Ha, M. Y. & Yoon, H. S. A numerical study of natural convection in a square enclosure with a circular cylinder at different vertical locations. *Int. J. Heat Mass Transf.* **51**, 1888–1906 (2008).
43. Khanafer, K., Vafai, K. & Lightstone, M. Buoyancy-driven heat transfer enhancement in a two-dimensional enclosure utilizing nanofluids. *Int. J. Heat Mass Transfer* **46**, 3639–3653 (2003).
44. Sheikholeslami, M. Lattice Boltzmann Method simulation of MHD non-Darcy nanofluid free convection. *Physica B* **516**, 55–71 (2017).
45. Anantha Kumar, K., Ramana Reddy, J. V., Sugunamma, V. & Sandeep, N. Magnetohydrodynamic Cattaneo-Christov flow past a cone and a wedge with variable heat source/sink. *Alexandria Engineering Journal* **57**, 435–443 (2018).
46. Kumar, K. A., Reddy, J. V. R., Vangala, S. & Sandeep, N. MHD flow of chemically reacting Williamson fluid over a curved/flat surface with variable heat source/sink, *International Journal of Fluid Mechanics Research*, https://doi.org/10.1615/InterJFluidMechRes.2018025940 (2018).
47. Anantha Kumar, K., Sugunamma, V. & Sandeep, N. Impact of non-linear radiation on MHD non-aligned stagnation point flow of micropolar fluid over a convective surface. *Journal of Non-Equilibrium Thermodynamics* **43**, 327–345 (2018).
48. Li, Z. *et al*. Solidification process through a solar energy storage enclosure using various sizes of Al2O3 nanoparticles. *Journal of Molecular Liquids* **275**, 941–954 (2019).
49. Bhagya Lakshmi, K., Anantha Kumar, K., Ramana Reddy, J. V. & Sugunamma, V. Influence of nonlinear radiation and cross diffusion on MHD flow of Casson and Walters-B nanofluids past a variable thickness sheet. *Journal of Nanofluids* **8**, 1–11, https://doi.org/10.1166/jon.2019.1564 (2019).
50. Raju, C. S. K. & Sandeep, N. Falkner Skan flow of a magnetic Carreau fluid past a wedge in the presence of cross diffusion. *European Physical Journal Plus* **131**, 267 (2016).
51. Sekhar, K. R. *et al.* Aligned magnetic dipole in nonlinear radiative Falkner-Skan flow of Casson fluid over a wedge containing suspension of nanoparticles and microorganisms. *International Journal of Nanoparticles* **9**(4), 213–233 (2017).

Author Contributions

M.I. and Z.S. modeled and solved the problem and wrote the manuscript. I.K. and A. Sh. thoroughly checked the mathematical modeling and English corrections. Z.S. contributed in the results and discussions. All the corresponding authors finalized the manuscript after its internal evaluation.

Additional Information

Competing Interests: The authors declare no competing interests.

Publisher's note: Springer Nature remains neutral with regard to jurisdictional claims in published maps and institutional affiliations.